

# A monolithic fluid–structure interaction solver Verification and Validation Application: venous valve motion

Chen-Yu CHIANG

O. Pironneau, T.W.H. Sheu, M. Thiriet

Laboratoire Jacques-Louis Lions (LJLL), Sorbonne U.  
Scientific Computing and Cardiovascular Simulation (SCCS) Lab, NTU

FreeFem++ days 2017

# Outline

- 1 3D monolithic formulation
- 2 Validation and Verificatoin
- 3 Computational contact
- 4 Future work

# Formulation of coupled system

## A general fluid-structure coupled system

### General Laws of Continuum Mechanics

$$\rho \left( \frac{\partial \mathbf{u}}{\partial t} + \mathbf{u} \cdot (\nabla \mathbf{u}) \right) = \nabla \cdot (\boldsymbol{\sigma}) + \mathbf{f} \quad (1)$$

For Newtonian incompressible fluid :  $\boldsymbol{\sigma}_f = -p^f \mathbf{I} + \mu \mathbf{D}$

For hyperelastic incompressible material :  $\boldsymbol{\sigma}_s = -p^s \mathbf{I} + \partial_{\mathbf{F}} \Psi \mathbf{F}^T$

For hyperelastic compressible material :  $\boldsymbol{\sigma}_s = J^{-1} \partial_{\mathbf{F}} \Psi \mathbf{F}^T$

$$\mathbf{D} = (\nabla \mathbf{u} + \nabla \mathbf{u}^T)$$

$\mathbf{X} : \Omega_0 \times (0, T) \mapsto \Omega_t : \mathbf{X}(x^0, t)$ : Lagrangian position at  $t$  of  $x^0$

$\mathbf{d} = \mathbf{X}(x^0, t) - x^0$ : displacement

$\mathbf{F}_{i,j} = \partial_{x_j^0} \mathbf{X}_i$ ;  $x_j^0$ : original position

$J = \det \mathbf{F}$ , the Jacobian of the deformation

# Hyperelastic material model

## Mooney–Rivlin model

$$\Psi(\mathbf{F}) = c_1 \text{tr}_{\mathbf{F}^T \mathbf{F}} + c_2 \left( \text{tr}_{(\mathbf{F}^T \mathbf{F})^2} - \text{tr}_{\mathbf{F}^T \mathbf{F}}^2 \right)$$

$$\partial_{\mathbf{F}} \Psi \mathbf{F}^T = (2c_1 - 4c_2 \text{tr}_{\mathbf{B}}) \mathbf{B} + 4c_2 \mathbf{B}^2, \quad \text{where } \mathbf{B} = \mathbf{F} \mathbf{F}^T. \quad (2)$$

## S<sup>t</sup>–Venant–Kirchhoff model

$$\Psi(\mathbf{F}) = \frac{\lambda_s}{2} \text{tr}_{\mathbf{E}}^2 + \mu_s \text{tr}_{\mathbf{E}^2}, \quad \mathbf{E} = \frac{1}{2} (\mathbf{F}^T \mathbf{F} - \mathbf{I})$$

$$\partial_{\mathbf{F}} \Psi \mathbf{F}^T = \left[ \lambda_s \left( \frac{\text{tr}_{\mathbf{B}}}{2} - \frac{3}{2} \right) - \mu_s \right] \mathbf{B} + \mu_s \mathbf{B}^2 \quad (3)$$

# Lagrangian points $(x^0, t)$ to Eulerian points $(x, t)$

$$\mathbf{F}^T = \nabla_{x^0} \mathbf{X} = \nabla_{x^0} (\mathbf{d} + x^0) = \nabla_{x^0} \mathbf{d} + \mathbf{I} = \mathbf{F}^T \nabla \mathbf{d} + \mathbf{I} \Rightarrow \mathbf{F} = (\mathbf{I} - \nabla \mathbf{d})^{-T}$$

$$\mathbf{C} = \mathbf{I} - \mathbf{B} = \mathbf{D} \mathbf{d} - \nabla \mathbf{d} \nabla^T \mathbf{d}$$

## Cayley–Hamilton theorem

For a general  $n \times n$  **invertible matrix**  $\mathbf{A}$ , i.e., one with nonzero determinant,  $\mathbf{A}^{-1}$  can thus be written as a  $n^{\text{th}}$  order polynomial expression in  $\mathbf{A}$

$$n = 3, \quad \mathbf{A}^3 - \text{tr}_{\mathbf{A}} \mathbf{A}^2 + \frac{1}{2} (\text{tr}_{\mathbf{A}}^2 - \text{tr}_{\mathbf{A}^2}) \mathbf{A} - \det_{\mathbf{A}} \mathbf{I} = 0$$

$n=3$

$$\begin{aligned} \mathbf{B} &= \text{tr}_{\mathbf{B}} \mathbf{I} - \frac{1}{2} (\text{tr}_{\mathbf{B}}^2 - \text{tr}_{\mathbf{B}^2}) \mathbf{B}^{-1} + J^2 \mathbf{B}^{-2}, \\ \mathbf{B}^2 &= \frac{1}{2} (\text{tr}_{\mathbf{B}}^2 + \text{tr}_{\mathbf{B}^2}) \mathbf{I} + \left[ J^2 - \frac{1}{2} (\text{tr}_{\mathbf{B}}^3 - \text{tr}_{\mathbf{B}} \text{tr}_{\mathbf{B}^2}) \right] \mathbf{B}^{-1} + \text{tr}_{\mathbf{B}} J^2 \mathbf{B}^{-2} \end{aligned} \quad (4)$$

# Stress tensor for hyperelastic models ( $n=3$ )

## Mooney–Rivlin model

$$\partial_{\mathbf{F}} \Psi \mathbf{F}^T = 2c_1 (\mathbf{D}\mathbf{d} - \nabla \mathbf{d} \nabla^T \mathbf{d})^2 + 2c_3 (\mathbf{D}\mathbf{d} - \nabla \mathbf{d} \nabla^T \mathbf{d}) + \alpha \mathbf{I} \quad (5)$$

$$c_3 := \frac{c_1}{2} (\text{tr}_{\mathbf{B}}^2 - \text{tr}_{\mathbf{B}^2} - 4) - 2c_2$$

## S<sup>t</sup>–Venant–Kirchhoff model

$$\partial_{\mathbf{F}} \Psi \mathbf{F}^T = \alpha \mathbf{I} + \beta (\mathbf{D}\mathbf{d} - \nabla \mathbf{d} \nabla^T \mathbf{d}) + \gamma (\mathbf{D}\mathbf{d} - \nabla \mathbf{d} \nabla^T \mathbf{d})^2 \quad (6)$$

$$\begin{cases} \alpha = \frac{\lambda_s}{4} (\text{tr}_{\mathbf{B}} - 3) (2\text{tr}_{\mathbf{B}} - \text{tr}_{\mathbf{B}}^2 + \text{tr}_{\mathbf{B}^2} + 2J^2) + \frac{\mu_s}{2} \text{tr}_{\mathbf{B}} (2\text{tr}_{\mathbf{B}} + \text{tr}_{\mathbf{B}^2} - \text{tr}_{\mathbf{B}}^2 - 2 + 2J^2) \\ \beta = \frac{\lambda_s}{4} (\text{tr}_{\mathbf{B}} - 3) (\text{tr}_{\mathbf{B}}^2 - \text{tr}_{\mathbf{B}^2} - 4J^2) + \frac{\mu_s}{2} (\text{tr}_{\mathbf{B}}^3 - \text{tr}_{\mathbf{B}} \text{tr}_{\mathbf{B}^2} - \text{tr}_{\mathbf{B}}^2 + \text{tr}_{\mathbf{B}^2} + 2J^2 - 4\text{tr}_{\mathbf{B}} J^2) \\ \gamma = \frac{\lambda_s}{2} (\text{tr}_{\mathbf{B}} - 3) J^2 + \mu_s (\text{tr}_{\mathbf{B}} - 1) J^2 \end{cases}$$

## Variational formulation (n=3)

$$\int_{\Omega_f^t} \left( \rho_f \mathbb{D}_t \mathbf{u} \cdot \hat{\mathbf{u}} + \frac{\mu}{2} \mathbf{D}\mathbf{u} : \mathbf{D}\hat{\mathbf{u}} - p \nabla \cdot \hat{\mathbf{u}} - \hat{p} \nabla \cdot \mathbf{u} \right) \\ + \int_{\Omega_s^t} \left[ \rho_s \mathbb{D}_t \mathbf{u} \cdot \hat{\mathbf{u}} + \frac{\gamma}{2} \left( \mathbf{D}\mathbf{d} - \nabla \mathbf{d} \nabla^T \mathbf{d} \right)^2 : \mathbf{D}\hat{\mathbf{u}} \right. \\ \left. + \frac{\beta}{2} \left( \mathbf{D}\mathbf{d} - \nabla \mathbf{d} \nabla^T \mathbf{d} \right) : \mathbf{D}\hat{\mathbf{u}} + \alpha \nabla \cdot \hat{\mathbf{u}} \right] = \int_{\Omega^t} \mathbf{f} \cdot \hat{\mathbf{u}} \quad (7)$$

$$\mathbb{D}_t \mathbf{d} = \mathbf{u}, \quad (8)$$

For simplicity,

- homogeneous boundary conditions on  $\Gamma \subset \partial\Omega$
- homogeneous Neumann conditions on  $\partial\Omega^t \setminus \Gamma$ .

So, given  $\Omega_f^0$ ,  $\Omega_s^0$ ,  $\mathbf{d}$ , and  $\mathbf{u}$  at  $t = 0$ , we must find

$(\mathbf{u}, p, \mathbf{d}, \Omega_f^t, \Omega_s^t)$  with  $\mathbf{u}|_\Gamma = 0$  and equation (7) and (8)

# A first order in time consistent approximation

Find  $\Omega^{n+1}, \mathbf{u}^{n+1} \in \mathbf{H}_0^1(\Omega^{n+1}), p^{n+1} \in L_0^2(\Omega^{n+1})$  such that for all  
 $\hat{\mathbf{u}}^{n+1} \in \mathbf{H}_0^1(\Omega^{n+1}), \hat{p}^{n+1} \in L_0^2(\Omega^{n+1}),$

$$\begin{aligned}
 & \int_{\Omega^{n+1}} \rho^{n+1} \frac{\mathbf{u}^{n+1} - \mathbf{u}^n \circ \mathbb{Y}^{n+1}}{\delta t} \cdot \hat{\mathbf{u}} + \int_{\Omega_f^{n+1}} \left( -p^{n+1} \nabla \cdot \hat{\mathbf{u}} - \hat{p} \nabla \cdot \mathbf{u} \frac{\mu}{2} \mathbf{D}\mathbf{u}^{n+1} : \mathbf{D}\hat{\mathbf{u}} \right) \\
 & + \delta t \int_{\Omega_s^{n+1}} \left[ \gamma^{n+1} \left( \mathbf{D}\mathbf{u}^{n+1} - \nabla \mathbf{u}^{n+1} \nabla^T \tilde{\mathbf{d}}^n - \nabla \tilde{\mathbf{d}}^n \nabla^T \mathbf{u}^{n+1} \right) \left( \mathbf{D}\tilde{\mathbf{d}}^n - \nabla \tilde{\mathbf{d}}^n \nabla^T \tilde{\mathbf{d}}^n \right) \right. \\
 & \quad \left. + \frac{\beta^{n+1}}{2} \left( \mathbf{D}\mathbf{u}^{n+1} - \nabla \mathbf{u}^{n+1} \nabla^T \tilde{\mathbf{d}}^n - \nabla \tilde{\mathbf{d}}^n \nabla^T \mathbf{u}^{n+1} \right) \right] : \mathbf{D}\hat{\mathbf{u}} \\
 & + \int_{\Omega_s^{n+1}} \left[ \frac{\gamma^{n+1}}{2} \left( \mathbf{D}\tilde{\mathbf{d}}^n - \nabla \tilde{\mathbf{d}}^n \nabla^T \tilde{\mathbf{d}}^n \right)^2 : \mathbf{D}\hat{\mathbf{u}} + \frac{\beta^{n+1}}{2} \left( \mathbf{D}\tilde{\mathbf{d}}^n - \nabla \tilde{\mathbf{d}}^n \nabla^T \tilde{\mathbf{d}}^n \right) : \mathbf{D}\hat{\mathbf{u}} \right. \\
 & \quad \left. + \alpha^{n+1} \nabla \cdot \hat{\mathbf{u}} \right] = \int_{\Omega^{n+1}} \mathbf{f} \cdot \hat{\mathbf{u}}
 \end{aligned} \tag{9}$$

where  $\tilde{\mathbf{d}}^n$  stands for  $\mathbf{d}^n(\mathbb{Y}^{n+1})$  and where  $\mathbf{d}^n$  is updated by

$$\mathbf{d}^{n+1} = \mathbf{d}^n \circ \mathbb{Y}^{n+1} + \delta t \mathbf{u}^{n+1} \tag{10}$$

# Solution algorithm

## Fixed point iteration

- ① Set  $\rho = \rho^n, \alpha = \alpha^n, \beta = \beta^n, \gamma = \gamma^n, \Omega = \Omega^n, \mathbf{u} = \mathbf{u}_h^n, \mathbb{Y}(x) = x - \mathbf{u}\delta t,$
- ② Solve equation (9),
- ③ Set  $\mathbf{u} = \mathbf{u}_h^{n+1}, \mathbb{Y}(x) = x - \mathbf{u}\delta t, \Omega_r = \mathbb{Y}^{-1}(\Omega_r^n), r = s, f,$  update  $\alpha, \beta, \gamma$  and  $\rho.$
- ④ If not converged return to step 2.

# Outline

## 1 3D monolithic formulation

## 2 Validation and Verificatoin

- A thin elastic plate clamped into a small rigid square body immersed in a flowing fluid
- A thin elastic plate clamped into a rigid cylinder immersed in a flowing fluid
- A rotatable cylinder and a flexible tail with a rear mass
- Bending of a flexible plate in cross flow
- Elastic structure in merging flow from two inlets

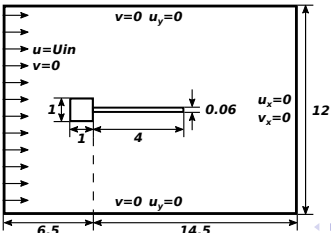
## 3 Computational contact

## 4 Future work

# A thin elastic plate clamped into a small rigid square body immersed in a flowing fluid

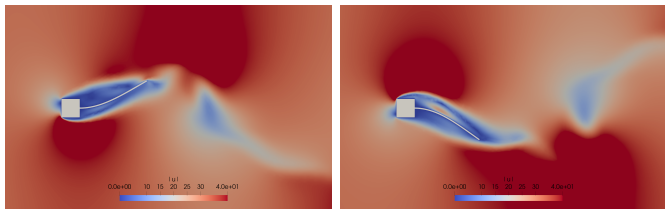
Table: Material parameters

$\rho_f \left[ g \text{ cm}^{-3} \right]$	$\nu_f \left[ g \text{ cm}^{-1} \text{s}^{-1} \right]$	$\rho_s \left[ g \text{ cm}^{-3} \right]$	$E \left[ g \text{ cm}^{-1} \text{s}^{-2} \right]$	$U_{in} \left[ \text{cm s}^{-1} \right]$
$1.18 \times 10^{-3}$	$1.82 \times 10^{-4}$	2	$2 \times 10^6$	31.5



# A thin elastic plate clamped into a small rigid square body immersed in a flowing fluid

Author	magnitude	frequency
present, $h_{min} = 0.02$	1.85	1.2
present, $h_{min} = 0.015$	1.94	1.2
Hubner	2.0	0.8



(a)

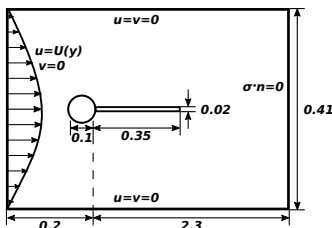
(b)

**Figure:** Contours of velocity magnitude at (a)  $t = 12.5$  and (b)  $t = 13.0$ .

## A thin elastic plate clamped into a rigid cylinder immersed in a flowing fluid

- Poiseuille profile inflow  

$$U(y) = 1.5U_{in} \frac{y(H-y)}{(0.5H)^2}$$
 and  $H = 0.41$
  - For fluid,  $\rho_f = 1000$  and  $\nu_f = 0.001$
  - Two steady cases,  $g_s = 2, 4$  and  $U_{in} = 0$   
 (structure  $\rho_s = 1000$  and  $E = 5 \times 10^5$ )
  - FSI1,  $U_{in} = 1$ ,  $\rho_s = 1000$  and  $E = 5 \times 10^5$
  - FSI2  $U_{in} = 2$ ,  $\rho_s = 10000$  and  $E = 2 \times 10^5$



	$g_s = 2$		$g_s = 4$	
	$d_x$	$d_y$	$d_x$	$d_y$
Present $h_{min} = 0.008$	7.179	65.82	24.84	120.82
Dunne [?]	7.187	66.10	-	-
Hron and Turek [?]	7.187	66.10	-	-
Richter [?]	7.149	66.07	25.10	122.16
Wick [?]	7.150	64.90	25.33	122.30

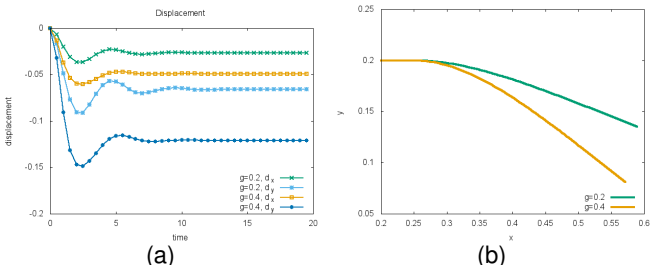


Figure: (a) displacement on  $x$  and  $y$  with respect to time, (b) centerlines position.

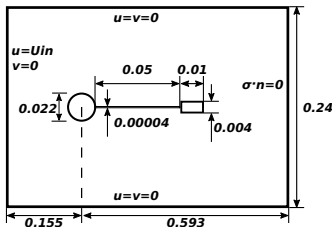
3D monolithic formulation  
**Validation and Verification**  
Computational contact  
Future work

A thin elastic plate clamped into a small rigid square body immersed in a flow  
A thin elastic plate clamped into a rigid cylinder immersed in a flow  
A rotatable cylinder and a flexible tail with a rear mass  
Bending of a flexible plate in cross flow  
Elastic structure in merging flow from two inlets

	FSI2		FSI3	
	amplitude	frequency	amplitude	frequency
Present $h_{min} = 0.004$	$7.61 \times 10^{-2}$	$2.03 s^{-1}$	$2.80 \times 10^{-2}$	$5.15 s^{-1}$
Present $h_{min} = 0.002$	$7.75 \times 10^{-2}$	$2.03 s^{-1}$	$3.01 \times 10^{-2}$	$5.18 s^{-1}$
Turek [?]	$8.06 \times 10^{-2}$	-	$3.44 \times 10^{-2}$	-
Dune [?]	$8.00 \times 10^{-2}$	$1.953 s^{-1}$	$3.00 \times 10^{-2}$	$5.04 s^{-1}$
Thomas [?]	$8.06 \times 10^{-2}$	$1.93 s^{-1}$	-	-

# A rotatable cylinder and a flexible tail with a rear mass

- $U_{in} = 1.07$
- Whole solid system flaps due to instability of wake region.
- Front cylinder rotates at frequency of 6.38 Hz and 7.35 Hz, experimentally and numerically determined value.
- Origin of coordinate is placed at center of cylinder.
- Measure points A and B locate at (0.082, 0) and (0.082, 0.04).

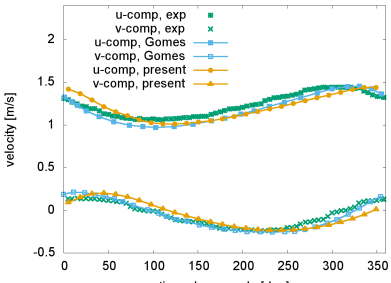
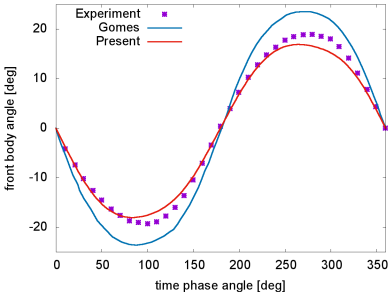
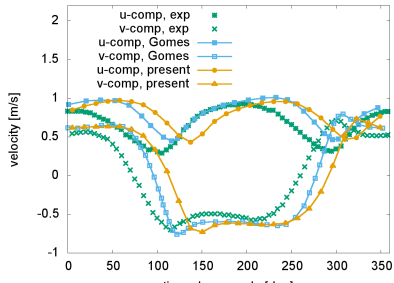
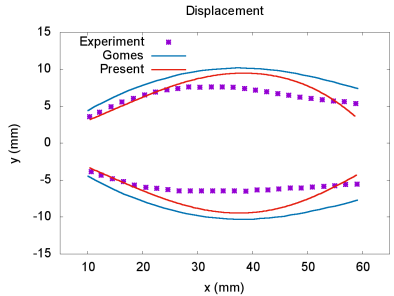


3D monolithic formulation  
**Validation and Verification**  
Computational contact  
Future work

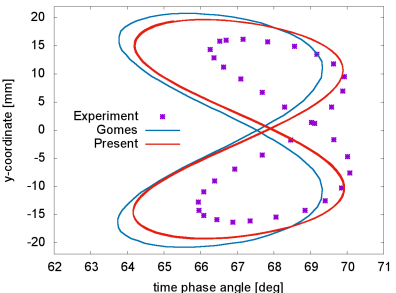
A thin elastic plate clamped into a small rigid square body immersed in a flow  
A thin elastic plate clamped into a rigid cylinder immersed in a flow  
**A rotatable cylinder and a flexible tail with a rear mass**  
Bending of a flexible plate in cross flow  
Elastic structure in merging flow from two inlets

3D monolithic formulation  
 Validation and Verification  
 Computational contact  
 Future work

A thin elastic plate clamped into a small rigid square body immersed in a flow  
 A thin elastic plate clamped into a rigid cylinder immersed in a flow  
 A rotatable cylinder and a flexible tail with a rear mass  
 Bending of a flexible plate in cross flow  
 Elastic structure in merging flow from two inlets

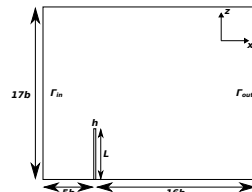
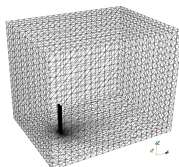


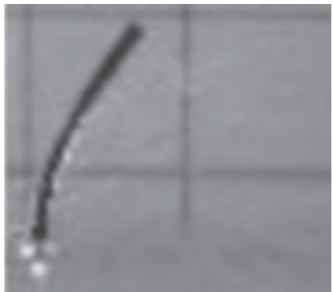
- Relatively good agreement in displacement, frequency and velocity at measure points.
- 30000 elements (P1b,P1), and first order in time.



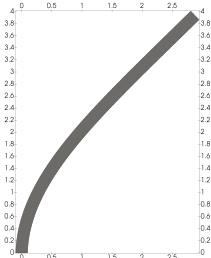
# Bending of a flexible plate in cross flow

- An elastic plate  $\left[-\frac{h}{2}, \frac{h}{2}\right] \times \left[-\frac{b}{2}, \frac{b}{2}\right] \times [0, L]$  is clamped to a rectangular tube  $[-5b, 16b] \times [-8b, 8b] \times [0, 17b]$
  - $h/b = 0.2$  and  $L/b = 5$
  - A constant inflow  $U_{in} = 1$  along  $x$  direction at  $\Gamma_{in}$
  - $Re = \frac{U_{in}b}{\nu} = 1600$  and  $\rho_f^* = 1$
  - $\rho_s^* = 0.678$ ,  $E^* = 19054.9$ , and  $\nu_s = 0.4$
  - Buoyancy force of solid  $f_h^* = 0.2465$





(a)



(b)

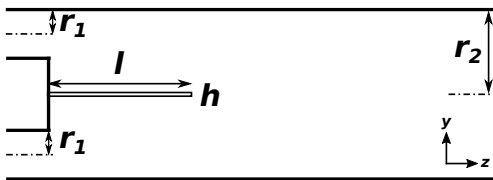
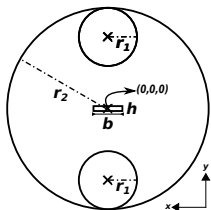
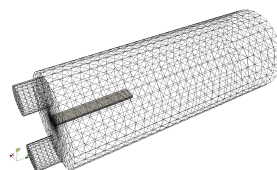
**Figure:** Bending of a flexible plate in cross flow. (a) Experimental results [?], (b) computational results.

	$C_D$	$\mathbf{D}_x/b$	$\mathbf{D}_z/b$
Present	1.03	2.13	0.54
Luhar and Nepf [?]	1.15 (with 10% error)	2.14	0.59
Tian and Dai etc [?]	1.03	2.12	0.54

**Table:** Comparison of drag coefficient  $C_D$  and deflection in  $x-$  and  $z-$  direction with respect to referenced data.

# Elastic structure in merging flow from two inlets

- A cylindrical chamber with  $r_2 = 76.2$  and length of 200
  - Two inlet pipes with  $r_1 = 21.0$  and length of 20
  - A silicon filament with  $h = 2$  thick,  $b = 11$  wide, and  $l = 65$  long
  - $\rho_f = 1.1633 \times 10^{-3}$  and  $\nu_f = 12.5 \times 10^{-3}$
  - $\rho_s = 1.0583 \times 10^{-3}$ , Young's modulus  $E_s = 216260$ , and Poisson ratio  $\nu_s = 0.315$
  - Gravity  $g = -9810$  along y direction



# Initial configuration due to buoyancy force

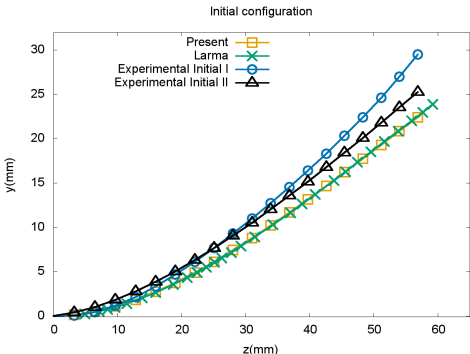
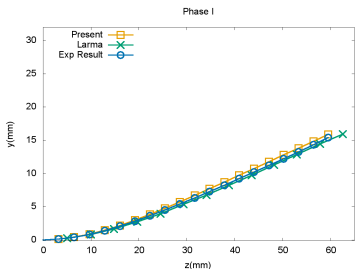


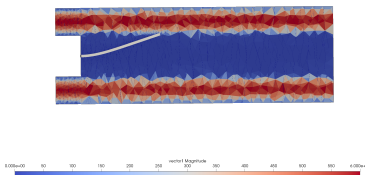
Figure: Initial deflection of silicone filament because of buoyancy force.

## Case I : steady deformation

Inlet velocity are Poiseuille profile with peak velocity of 630 and 615 for upper and lower inlet respectively.



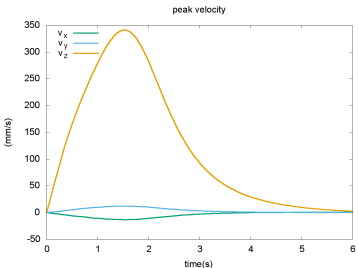
(a)



(b)

Figure: Computational results for phase I (a) position of center line along  $z$  direction, (b) velocity profiles at symmetric plane  $x = 0$ .

## Case II : starting flow



	$n_1$	$n_2$	$n_3$	$d_0$	$b_1$	$b_2$	$b_3$	$b_4$	$\hat{l}_k$
$\hat{v}_x$	-11.37	-28.99	7.73	1.38	0.24	3.59	-3.14	1	[0, 4.07]
$\hat{v}_y$	14.95	11.88	-2.17	2.06	-2.0	4.95	-3.50	1	[0, 5.51]
$\hat{v}_z$	367.10	363.40	-62.24	1.21	-0.38	3.76	-3.19	1	[0, 5.27]

**Table:** For case II, curve-fitting coefficients of inlet peak velocity for  $\hat{v}_k(t) = \sum_{i=1}^3 n_i t^i / \sum_{j=0}^4 b_j t^j$  with  $\hat{v}_k = 0$  for  $t \in \mathbb{I} \setminus \hat{l}_k$ . Note, that flow in  $y$  direction is applied only in the upper inlet.

3D monolithic formulation  
Validation and Verification  
Computational contact  
Future work

A thin elastic plate clamped into a small rigid square body immersed in a flow  
A thin elastic plate clamped into a rigid cylinder immersed in a flowing fluid  
A rotatable cylinder and a flexible tail with a rear mass  
Bending of a flexible plate in cross flow  
Elastic structure in merging flow from two inlets

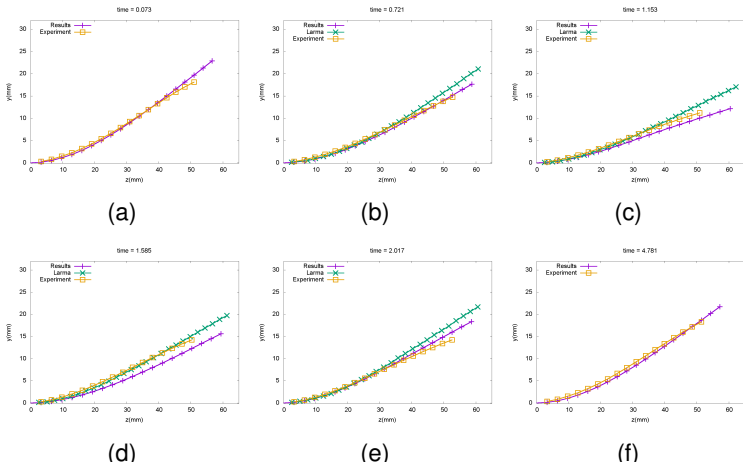
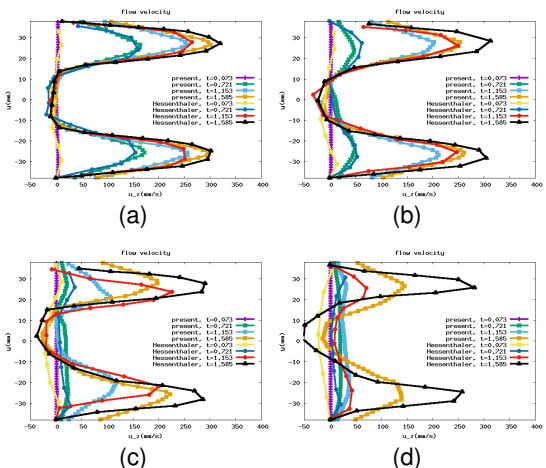


Figure: Deflection of the silicone filament in phase II (a)  $t = 0.073$ , (b)  $t = 0.721$ , (c)  $t = 1.153$ , (d)  $t = 1.585$ , (e)  $t = 2.017$ , (f)  $t = 4.781$ .

# 3D monolithic formulation Validation and Verification Computational contact Future work

- A thin elastic plate clamped into a small rigid square body immersed
- A thin elastic plate clamped into a rigid cylinder immersed in a flow
- A rotatable cylinder and a flexible tail with a rear mass
- Bending of a flexible plate in cross flow
- Elastic structure in merging flow from two inlets



**Figure:** At midplane  $x = 0$  mm, flow velocity component  $u_z$  at (a)  $z \approx 0.20l$ , (b)  $z \approx 0.51l$ , (c)  $z \approx 0.82l$ , (d)  $z \approx 1.12l$  ( $l = 65$  mm, length of the silicon filament).

# Outline

- 1 3D monolithic formulation
- 2 Validation and Verificatoin
- 3 Computational contact
  - Variational inequality/constrain for contact
  - Valved veins
- 4 Future work

# Computational contact

## Variational inequality/constrain for contact

$$A(\mathbf{u}, \mathbf{v}) + \Lambda(\mathbf{u}, \mathbf{v}) = b(\mathbf{v})$$

where  $\Lambda$  is a variational constrain for contact

$$\Lambda(\mathbf{u}, \mathbf{v}) = \int_{\partial\Omega^t} \lambda \mathbf{n} \cdot \mathbf{v}, \quad \begin{cases} \lambda(\mathbf{x}, t) \leq 0, \quad \forall \mathbf{x}, \\ d_{S_i^t}(\mathbf{x}) \lambda(\mathbf{x}, t) = 0, \quad \forall \mathbf{x} \in S_i^t \end{cases}$$

To each simply connected disjointed part  $S_i^t$ ,  $i = 1 \dots n_s$  is associated a signed distance function  $\mathbf{x} \mapsto d_{S_i^t}$  measuring distance of  $\mathbf{x}$  to  $S_i^t$ .

$$\begin{cases} d_{S_i^t} < 0, & \text{structure region} \\ d_{S_i^t} = 0, & \text{contact point/line/surface} \quad \text{for some } \mathbf{x} \in \partial\Omega/S_i^t \\ d_{S_i^t} > 0, & \text{fluid region} \end{cases}$$

# Computational contact

## Semi-Smooth Newton Method

In  $k^{th}$  iteration for each time step  $n + 1$

$$\lambda^{n+1,k+1} = \min \left\{ 0, \lambda^{n+1,k} + c_0 d_{S_i^t} \left( \mathbf{x} + \delta t \mathbf{u}^{n+1,k} \right) \right\}. \forall \mathbf{x} \in S_i^{n+1}$$

Original equations can be recast into

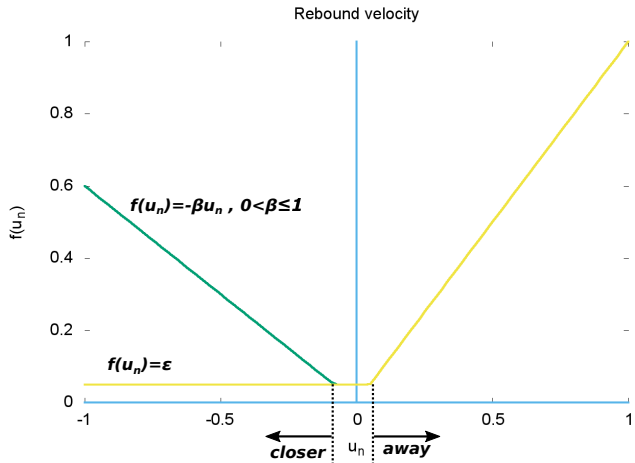
$$A(\mathbf{u}^{n+1,k+1}, \mathbf{v}) + \tau_{ck} G(\mathbf{u}^{n+1,k+1}, \mathbf{v}) = b(\mathbf{v})$$

$$G(\mathbf{u}^{n+1,k+1}, \mathbf{v}) = \sum_{i=1}^{n_s} \int_{S_{n+1}^i \cap \left\{ \mathbf{x}: \lambda^{n+1,k} + c_0 d_{S_{n+1}^i} (\mathbf{x} + \delta t \mathbf{u}^{n+1,k}) \right\}} g(\mathbf{u}^{n+1,k+1}, \mathbf{v})$$

where function  $f$  is associated to rebound velocity and variant with different model.

# Rebound velocity

For example  $g(\mathbf{u}^{n+1,k+1}) = \mathbf{u}^{n+1,k+1} - f(\mathbf{u}^{n+1,k} \cdot \mathbf{n}) \mathbf{n}$



3D monolithic formulation  
Validation and Verification  
**Computational contact**  
Future work

Variational inequality/constraint for contact  
Valved veins

# Free falling ball hit a slope

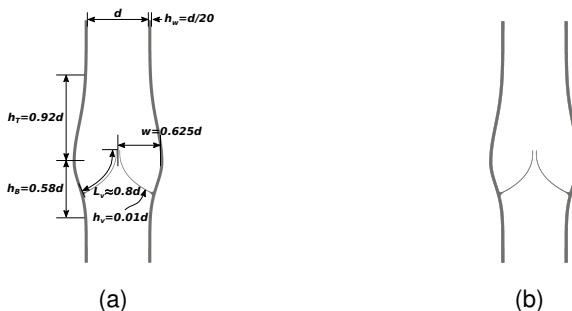


Figure: Shape and size of one valved vein

3D monolithic formulation  
Validation and Verification  
**Computational contact**  
Future work

Variational inequality/constraint for contact  
Valved veins

3D monolithic formulation  
Validation and Verification  
**Computational contact**  
Future work

Variational inequality/constraint for contact  
Valved veins

# Outline

- 1 3D monolithic formulation
- 2 Validation and Verificatoin
- 3 Computational contact
- 4 Future work

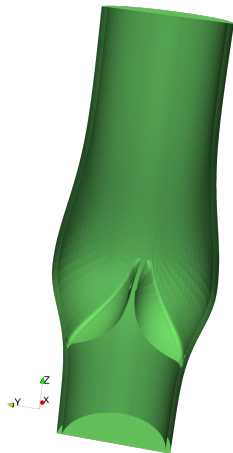
## Modeling

- In/out-let boundary conditions of blood vessels
- Anisotropic hyperelastic material model for vascular walls and valves
- Model for aggregation and deformation of red blood capsules

## Simulation

- Parallelize whole computational process with domain decomposition method
- Vascular model and simulation in 3D
- Comparison with experimental data

Thanks for your listening.



# Flow rate and volume

